Scoliosis imaging : an analysis of radiation risk in the CT scan projection radiograph and a comparison with projection radiography and EOS

Alrehily, F, Hogg, P, Twiste, M, Johansen, S and Tootell, AK

http://dx.doi.org/10.1016/j.radi.2019.02.005

Scoliosis imaging: an analysis of radiation risk in the CT Scan Projection Radiograph and a comparison with projection radiography and EOS

Faisal Alrehily [1,2]

Peter Hogg [2]

Martin Twiste [2]

Safora Johansen [3,4]

Andrew Tootell [2]

1 College of Applied Medical Sciences, Taibah University, Medina 42353, Saudi Arabia

2 School of Health Sciences, University of Salford, Salford M5 4WT, United Kingdom.

3 Oslo Metropolitan University, Faculty of Health Sciences, Norway.

4 Department of Oncology, Division of Cancer Medicine, Surgery and Transplantation, Oslo University Hospital, Radiumhospitalet, Oslo, Norway.

Abstract

Introduction: Scoliosis is defined as a deformity of the spine with lateral curvature in the coronal plane. It requires regular X-ray imaging to monitor the progress of the disorder, therefore scoliotic patients are frequently exposed to radiation. It is important to lower the risk from these exposures for young patients. The aim of this work is to compare organ dose (OD) values resulting from Scan Projection Radiograph (SPR) mode in CT against projection radiography and EOS® imaging system when assessing scoliosis.

Methods: A dosimetry phantom was used to represent a 10-year old child. Thermoluminescent dosimetry detectors were used for measuring OD. The phantom was imaged with CT in SPR mode using 27 imaging parameters; projection radiography and EOS machines using local scoliosis imaging procedures. Imaging was performed in anteroposterior, posteroanterior and lateral projections.

Results: 17 protocols delivered significantly lower radiation dose than projection radiography ($p < 0.05$). OD values from the CT SPR imaging protocols and projection radiography were statistically significant higher than the results from EOS. No statistically significant differences in OD were observed between 10 imaging protocols and those from projection radiography and EOS imaging protocols ($p > 0.05$).

Conclusion: EOS has the lowest dose. Where this technology is not available we suggest there is a potential for OD reduction in scoliosis imaging using CT SPR compared to projection radiography. Further work is required to investigate image quality in relation to the measurement of Cobb angle with CT SPR

Introduction

Scoliosis is a medical condition in which the spine is abnormally twisted laterally. One of the most common types of scoliosis is adolescent idiopathic scoliosis (AIS), which predominantly affects young females rather than males [1,2]. Scoliosis requires regular X-ray imaging to monitor the progress of the disorder, therefore scoliotic patients are frequently exposed to radiation. Younger people are more prone to develop radiation-induced cancer; this is due to the length of time they can live post exposure and the rate of cell division [3]. Radiation cancer induction is also gender dependent, with females being more radiosensitive than males. Compared with the general public, the amount of ionising radiation young female patients receive during the management of scoliosis increases the risk of breast cancer occurrence by approximately 70% [4]. Knowing scoliosis is more prevalent in young females, there is a need to pay attention to dose optimisation in this subpopulation. Therefore, it is very important to select imaging technologies which offer lowest radiation dose consistent with the clinical requirements; and for those technologies there is a need to optimise dose and image quality to produce images which are fit for purpose.

The assessment of scoliosis can be performed using a range of imaging modalities which can be categorised as follows: (1) those utilising ionising radiation (e.g. projection radiography, EOS® (EOS imaging system, Paris, France) and CT); and (2) those using optical imaging with light (e.g. Diers International GmbH, Schlangenbad, Germany). For many years, projection radiography using general purpose X-ray machines has been the primary tool used to confirm the existence of scoliosis, to determine curvature severity and to monitor its progression and treatment success [1]. EOS® is one of the latest advances in orthopaedic imaging using ionising radiation. It uses low dose to produce 3D images of the spine by capturing, simultaneously, two X-ray images; anterior-posterior (AP) *or* posterior-anterior (PA) and lateral projections. The measurements from the reconstructed 3D images have been shown to have better inter-observer agreement than projection radiography[5]. In CT for scoliosis assessment, the Scan Projection Radiograph (SPR) image (without axial imaging) can be used to evaluate the spine. Sometimes referred to as the “scout view” or “scanogram”, SPR is the scanning mode in CT that is used prior to the clinical CT scan and it is used to set CT acquisition range and imaging parameters. SPR can generate AP, PA and lateral images.

Once acquired, the images can be used to measure Cobb angle; this angle gives an indication of spine curvature [6]. It is worth noting that X-ray imaging is usually performed while the

patient is erect as this accentuates scoliosis due to gravity. Conventional CT scanners, on the other hand, perform scans while the patient is lying on the table (i.e. supine or prone). This could lead to an underestimation of the Cobb angle, and hence to account for supine / prone imaging, a calculation can be performed to make a correction to the Cobb angle. As proven by Lee, Solomito and Patel, the correction allows for the supine measurement to represent the Cobb angle that would be attained in the erect position, with an acceptable error [7].

The aim of this article is to quantify organ dose from CT SPR when used to image the whole spine in a phantom and to compare it to radiation dose resulting from projection radiography and EOS acquisitions.

Method and materials

Organ doses (OD) of various organs, as listed in Table 1, were measured and Lifetime Attributable Risk (LAR) of cancer were calculated. This involved loading a dosimetry phantom (ATOM dosimeter phantom model 706) (CIRS Inc., Norfolk, Virginia, USA) (Figure 1), which represents a 10-year-old child, with Thermoluminescent dosimeters (TLD) (Harshaw TLD-100H (LiF: Mg, Cu, P)), to calculate the risk of radiation-induced cancer for both males and females. The ovaries, uterus, prostate and testes dose were measured; and because these organs are in different locations inside the phantom, it was possible to ignore the prostate and testes OD and calculate the risk for females. TLDs were calibrated and annealed prior to use as per published guidelines and literature [8,9]. The dosimetry phantom was irradiated using a CT scanner, conventional projection radiography machine and EOS imaging system. The mean of the organs' TLDs readings was calculated to give the absorbed organ dose. The active bone marrow dose was calculated using the weighted mean as described by Cristy [10].

Figure 1 The phantom on the CT table

Table 1: The organs that were assessed using phantom model 706 [11].						
Eyes	Brain	Thyroid	Heart	Thymus	Lung	Liver
Gall bladder	Spleen	Oesophagus	Stomach	Pancreas	Kidneys	Adrenals
Intestines	Ovaries	Uterus	Urinary bladder	Testes	Prostate	Active bone marrow

Imaging conditions

Prior to conducting the experiments, the EOS, CT and X-ray machine had undergone quality testing in accordance with IPEM report 91 [12], which relates primarily to imaging performance and radiation safety checks; results fell within manufacturer tolerances. The phantom was then irradiated using these machines as follows:

CT scan (SPR mode)

The phantom was placed on the imaging couch of a 3rd generation 16-slice CT scanner (Toshiba Aquillion; Toshiba Medical Systems, Japan) in a supine position with the head towards the gantry. The scan range was set to cover the area from the intersection between

vertebrae C3/C4 to the iliac crests [13]. Tape markers were placed onto the phantom and CT imaging couch to ensure the phantom was positioned in the same position for each exposure. Scan range was set to cover the area of interest; lateral alteration of the radiation field was not permitted in SPR mode. Twenty-seven SPR exposures were made in AP, PA, and lateral projections using combinations of 80, 100 and120 kVp and three mA values (10, 20 and 30 mA) (Table 2). CT exposure factors were selected based on the local guidelines for imaging an average 10-year old child at a local teaching hospital.

Projection radiography

The phantom was irradiated using a DigitalDiagnost X-ray imaging machine (Philips Healthcare, The Netherlands) at 85 kV for AP and PA projections and 90 kV for the lateral projection with automatic selection of the mAs (Figure 2). The source to image distance (SID) was 180 cm. The primary radiation field was set to cover the same area that was imaged using the CT SPR mode. Because the area of interest is large, the imaging system automatically divided the acquisition into an upper and lower region, hence two exposures were needed to capture the whole spine, which were then digitally stitched together post acquisition.

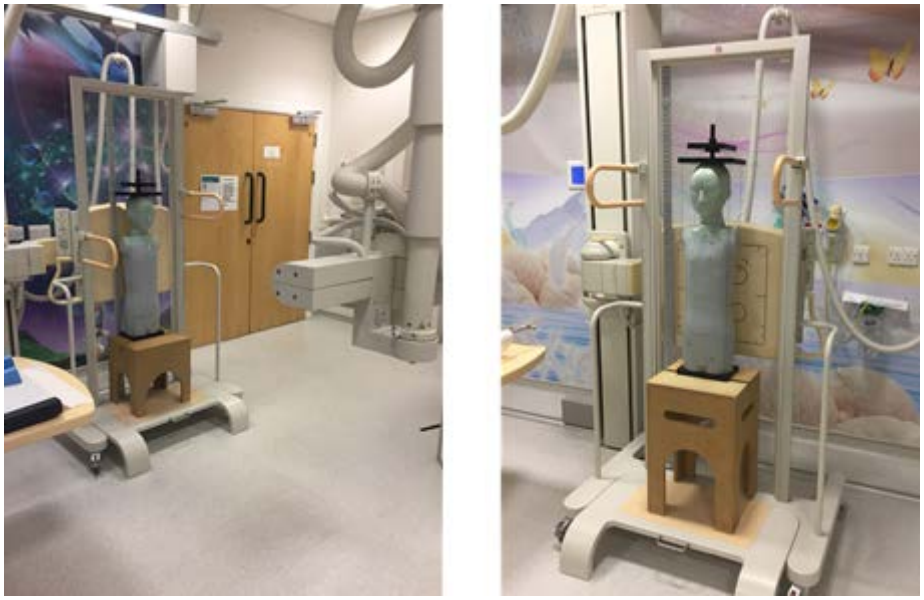

Figure 2: Shows the phantom while it is imaged using the conventional projection radiography imaging machines

EOS

The phantom was imaged using the EOS imaging system (Figure 3) and automatic exposure factors for an average 10-year-old child at a local teaching hospital (Table 4). It was then

irradiated in AP and lateral projections because the EOS can take two X-ray images from two sides (AP and lateral) simultaneously. Because the EOS can image from one side, projection imaging irradiation was made in AP and lateral separately.

Figure 3: The phantom inside an EOS imaging system. The light on both sides shows the postion of the X-ray tubes.

TLD dose readings and calculations

TLDs were read using Harshaw 3500 TLD reader (Thermo Scientific, USA) and the mean of the organs' TLDs were calculated to give the OD Equation 1.

$$OD_{organ} = \frac{\sum_n \ charge\ (nano\ columb) \times CF}{n} \qquad (1)$$

where CF is the calibration factor and n is the number of TLDs for that organ.

$$Lifetime\ attribuatble\ risk\ (LAR) = \sum_T r_T \times (OD_{organ} \times W_R) \qquad (2)$$

where r_T is the organ-specific radiation induced cancer factor of tissue (T) [14] and W_R is the radiation weighting factor (W_R for X-ray = 1).

Data analysis

Normality tests were performed on each set of data using the Shapiro-Wilk test. T-test and Wilcoxon test were used to determine the differences between organ doses of each imaging protocol. The data were processed using SPSS Statistics 23 (IBM Corp., New York).

Results

Table 2, Table 3 and Table 4 show the LAR from using the CT SPR mode, conventional projection radiography, and EOS imaging system.

Table 2: The LAR from using different SPR imaging protocols.

Imaging protocol	Imaging projection	Kilovoltage peak (kVp)	Tube current (mA)	LAR for 10-year-old female patient (per 10^6)	LAR for 10-year-old male patient (per 10^6)
CT1	AP	120	10	1.61	0.75
CT2	AP	120	20	3.07	1.35
CT3	AP	120	30	7.9	3.17
CT4	PA	120	10	0.50	0.24
CT5	PA	120	20	1.04	0.49
CT6	PA	120	30	3.10	1.40
CT7	AP	100	10	0.94	0.4
CT8	AP	100	20	1.81	0.82
CT9	AP	100	30	5.07	2.03
CT10	PA	100	10	0.3	0.13
CT11	PA	100	20	0.58	0.27
CT12	PA	100	30	1.9	0.85
CT13	AP	80	10	0.53	0.23
CT14	AP	80	20	0.9	0.34
CT15	AP	80	30	3	1.2
CT16	PA	80	10	0.14	0.06
CT17	PA	80	20	0.32	0.15
CT18	PA	80	30	0.91	0.41
CT19	Lateral	120	10	0.59	0.25
CT20	Lateral	120	20	1.03	0.47
CT21	Lateral	120	30	1.45	0.66
CT22	Lateral	100	10	0.31	0.13
CT23	Lateral	100	20	0.59	0.26
CT24	Lateral	100	30	0.88	0.40

CT25	Lateral	80	10	0.15	0.07
CT26	Lateral	80	20	0.31	0.13
CT27	Lateral	80	30	0.47	0.20

Table 3: The LAR from using conventional projection radiography machine,[1] refers to the upper image and [2] refers to the lower image

Imaging protocol	Imaging projections	Acquisition parameters		LAR for 10-year-old female patient (per 10^6)	LAR for 10-year-old male patient (per 10^6)
		kV	mAs		
X-ray1	AP_1	85	5.9	2.26	1.03
	AP_2	85	9.5		
X-ray2	PA_1	85	4.3	0.92	0.52
	PA_2	85	12.2		
X-ray3	$Lateral_1$	90	5	1.15	0.64
	$Lateral_2$	90	11		

Table 4: The LAR from using EOS imaging system. * means that these imaging projections were acquired simultaneously.

Imaging protocol	Imaging projections	Acquisition parameters		LAR for 10-year-old female patient (per 10^6)	LAR for 10-year-old male patient (per 10^6)
		kV	mA		
EOS1	AP *	75	200	0.86	0.37
	Lateral *	95	200		
EOS2	AP	75	200	0.25	0.09
EOS3	Lateral	80	80	0.07	0.03

Figures 4 - 7 show OD for heart, breast, lung and thymus as a sample from the overall OD data; these ODs are presented because they represent the largest OD values. In general, organs closer to the X-ray tube received a higher dose compared with organs that are located further away.

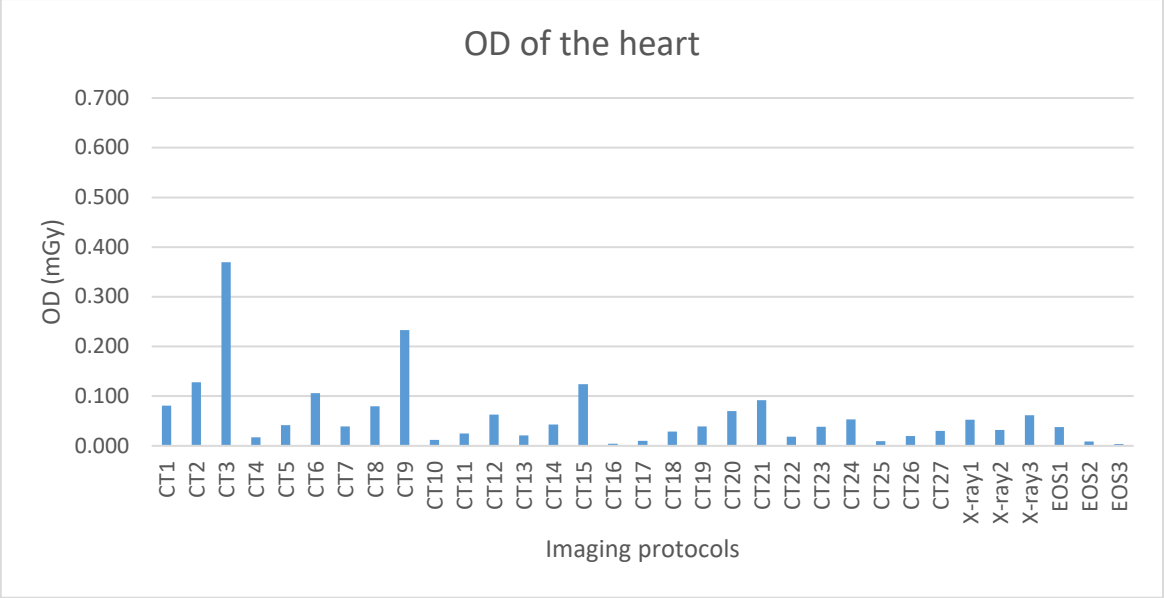

Figure 4: The OD of the heart from different imaging protocols.

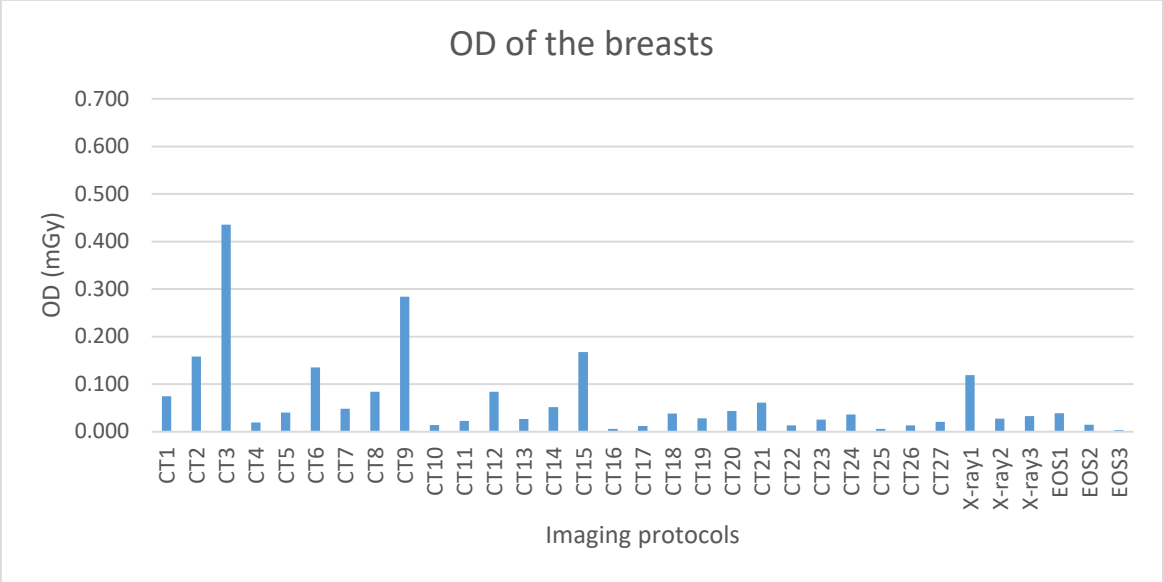

Figure 5: The OD of the breasts from different imaging protocols.

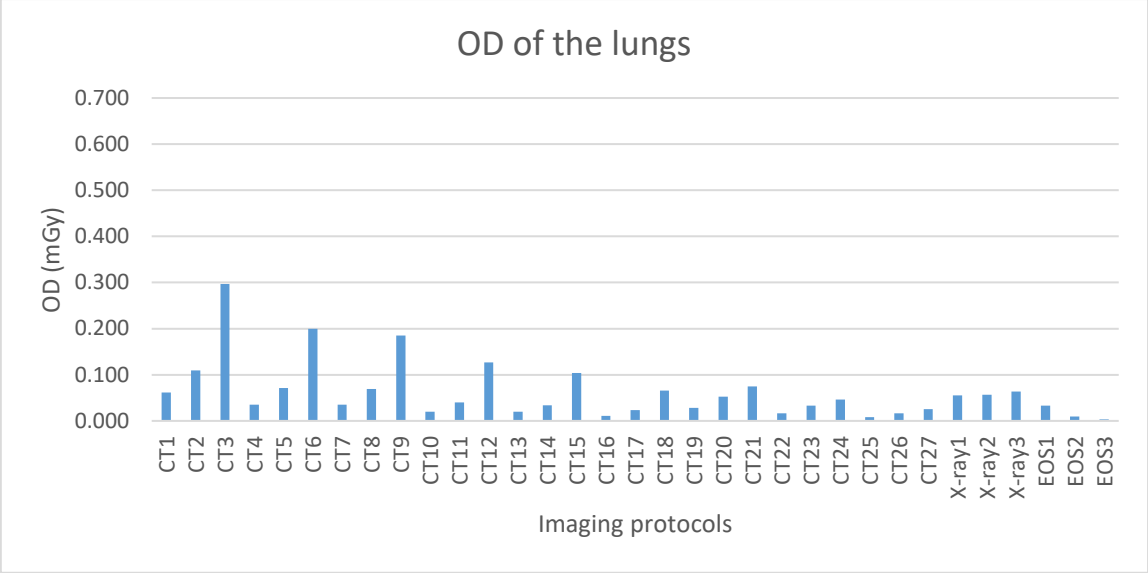

Figure 6: The OD of the lungs OD from different imaging protocols.

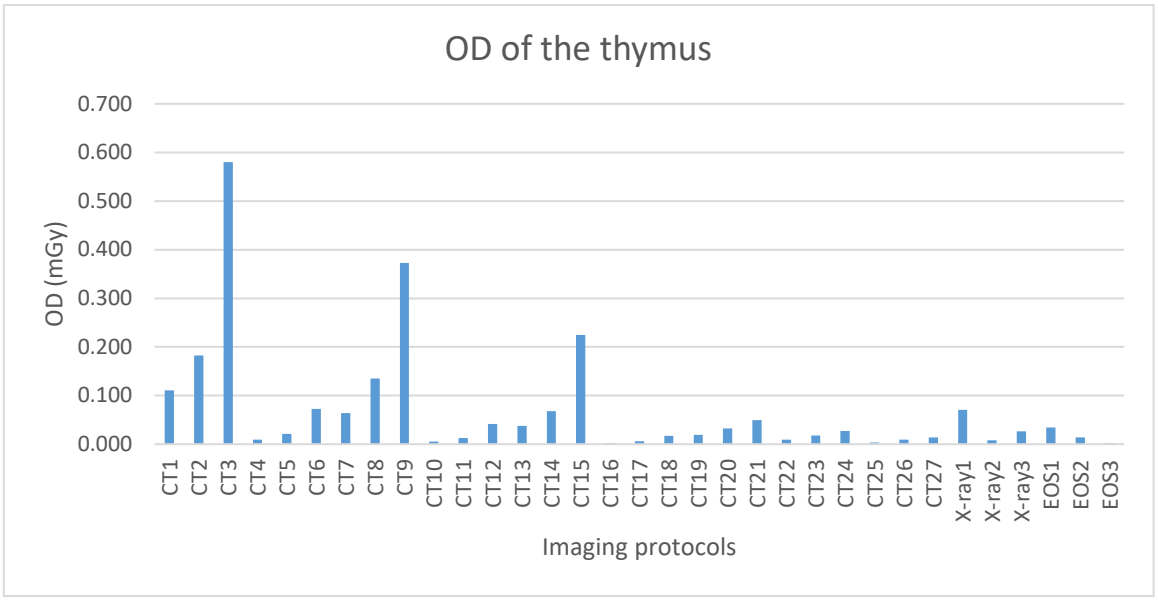

Figure 7: The OD of the thymus OD from different imaging protocols.

Table 5 shows SPR imaging protocols that deliver the same level of radiation compared with the imaging protocols that are currently used in practice (P>0.05). Table 6 shows SPR imaging protocols that deliver lower radiation dose when compared with projection radiography and EOS imaging protocols.

Table 5: SPR imaging protocols that deliver radiation dose equal to the ones from the most common imaging machines used for scoliosis assessment*.

Currently used protocols	**EOS2** (AP, 75, 200)	**X-ray1** (AP ,85, 5.9, 9.5)	**X-ray2** (PA, 85, 4.3, 12.2)	**X-ray3** (lateral, 90, 5, 11)
Proposed imaging protocols	CT1 (AP, 120, 10) CT2 (AP, 120, 20) CT5 (PA, 120, 20) CT11 (PA, 100, 20)	CT11 (PA, 100, 20) CT12 (PA, 100, 30) CT15 (AP, 80, 30)	CT4 (PA, 120, 10) CT8 (AP,100, 20) CT11 (PA,100, 20)	CT20 (Lateral, 120, 20) CT21 (Lateral, 120, 30)

* the Data in parenthesis state the imaging parameters as follow:

For CT imaging protocols (imaging projection, kVp, mA).

For X-ray imaging protocols (imaging projection, kV, mAs1, mAs2).

For EOS imaging protocols (imaging protocols, kV, mA).

Table 6: SPR imaging protocols that deliver radiation dose lower than the ones from the most common imaging machines used for scoliosis assessment*.

Currently used protocols	**X-ray1** (AP, 85, 5.9, 9.5)	**X-ray2** (PA, 85, 4.3, 12.2)	**X-ray3** (lateral, 90, 5, 11)
Proposed imaging protocols	CT1 (AP, 120, 10) CT4 (PA, 120, 10) CT5 (PA, 120, 20) CT7 (AP, 100, 10) CT8 (AP, 100, 20) CT10 (PA, 100, 10) CT13 (AP, 80, 10) CT14 (AP, 80, 20) CT16 (PA, 80, 10) CT17 (PA, 80, 20) CT18 (PA, 80, 30)	CT5 (PA, 120, 20) CT7 (AP, 100, 10) CT10 (PA, 100, 10) CT13 (AP, 80, 10) CT14 (AP, 80, 20) CT16 (PA, 80, 10) CT17 (PA, 80, 20) CT18 (PA, 80, 30)	CT19 (lateral, 120, 10) CT22 (lateral, 100, 10) CT23 (lateral, 100, 20) CT24 (lateral, 100, 30) CT25 (lateral, 80, 10) CT26 (lateral, 80, 20) CT27 (lateral, 80, 30)

* the Data in parenthesis state the imaging parameters as follow:

For CT imaging protocols (imaging projection, kVp, mA).

For X-ray imaging protocols (imaging projection, kV, mAs1, mAs2).

For EOS imaging protocols (imaging protocols, kV, mA).

Discussion

Patients with scoliosis often require frequent imaging to manage the condition; this means they are exposed to repeated ionising radiation exposures. This is concerning since scoliosis affects young females who have, compared with males and older people, a higher risk of developing radiation-induced cancer when exposed to radiation early in their life [15,16]. Our study found that CT SPR offers radiation reduction benefits when compared with projection radiography. However, when compared with EOS, SPR results in a higher radiation dose. Knowing that EOS systems are not as widely available as CT, a case might be made for imaging patients using SPR instead of projection radiography in centres that do not have EOS. However, there is a need to apply correction to any measurements of Cobb angle and recognition of any errors this may result in due to the non-weight-bearing acquisition.

The data show that imaging the spine in PA projection instead of AP can lower the overall OD. The reason for this is related to the lower energy X-rays being absorbed by the superficial organs in close proximity to primary beam entry point; as the beam progresses through the body it hardens thereby reducing the number of lower energy X-rays available for absorption [17]. This makes PA projection preferred for imaging scoliosis in females as it reduces breast dose and consequently reduces the risk of developing radiation-induced cancer [18]. However, few AP SPR imaging protocols (i.e. CT 7, 13, and 14) delivered lower radiation dose than imaging in PA using projection radiography. This could improve the appearance of the spine in the images because it is closer to image receptors, which means its appearance is less magnified and distorted.

A number of studies by Law et al have investigated the level of radiation when using projection radiography and EOS to assess scoliosis data from projection radiography [19–21]. For Law's work [19–21], to achieve study aims, they used modelling software (PCXMC) instead of direct measurements to estimate radiation dose level. Using PCXMC to calculate the OD is valid and reliable in terms of giving an estimation of radiation risk [22]. Moreover, using this type of calculation is easy to perform and not time consuming, which is another advantage in using the software. However, PCXMC cannot simulate non-flat radiation filters (e.g. bowtie filter) that are applied in most CT scanner [23]. Therefore, using direct measurement, as in our work, gives more precise determination of the OD and the LAR for several reasons. One limitation of using PCXMC is that the accuracy of the measurement is affected by the reproduced beam size and location [24]. Failing to use the exact same beam size and location

changes the outcomes of the calculation which may result in recording inaccurate outcomes. Another limitation is that the simulation software generates a uniform X-ray field which does not simulate the actual X-ray beam [25]. Lastly, the mathematical phantom that is used in the PCXMC software is scaled to match average population sizes. These limitations affect the accuracy of the measurements which can be overcome by using direct measurements (e.g. TLD).

CT scanners perform scans while the patient is lying on the table (i.e. supine or prone) while the gold standard for scoliosis imaging is weight-bearing. The upright position allows gravity to affect the morphology of the spine [26]. The value of the CT approach is limited because of the capability of CT scanners and their inability to perform weight-bearing imaging. Nonetheless, the validity of the patient lying on the table, and particularly in a supine position, to assess scoliosis has been proven by Lee, Solomito and Patel, who established a non-direct method to measure Cobb angle of the spine with acceptable range of error [7]. They proposed a new equation that allows converting measures from a magnetic resonance imaging (MRI) image to X-ray measures. On the other hand, Wessberg, Danielson and Willen found that Cobb angle measurements in a supine position are comparable to measurements in an upright position when using a supporting device (i.e. axial load device) [27]. Nevertheless, if proven to be a valid tool in terms of assessing scoliosis, the outcomes of our current work could be promising for patients and health providers. CT scanners are already available in most if not all hospitals, and hence no further investment in specialist imaging equipment, or additional staff training, is required

Conclusion

This paper is the first to investigate organ-specific doses using direct radiation measurement in CT SPR mode for imaging the spine for scoliosis assessment. Radiation risk from scoliosis imaging in young females can be lowered. This can be achieved by (1) using the EOS; (2) using PA projection rather than AP; (3) where EOS is not available using CT SPR with optimised protocols. For the latter, weight bearing CT is preferred but as availability is extremely limited, then a mathematical correction should be applied to supine-derived Cobb angle values.

Acknowledgments

We would like to thank Christie Medical Physics and Engineering department – The Christie NHS Foundation Trust for allowing us to use the phantom. We would also like to show our gratitude to Andrea Hulme from Manchester Children's Hospital and Emma McDonough from Alder Hey hospital for their assistance with imaging the phantom.

References

1. Kim H, Kim HS, Moon ES, et al. Scoliosis Imaging : What Radiologists Should Know. *Main*. 2010;30(2006):1823-1842. doi:10.1148/rg.307105061

2. Trobisch P, Suess O, Schwab F. Idiopathic scoliosis. *Dtsch Arztebl Int*. 2010;107(49):875-883; doi:10.3238/arztebl.2010.0875

3. Ng J, Shuryak I. Minimizing second cancer risk following radiotherapy: current perspectives. *Cancer Manag Res*. 2015;7:1-11. doi:10.2147/CMAR.S47220

4. Goethem V, M JW, Hauwe V, Luc, Parizel, M P. *Spinal Imaging*. Berlin: Springer; 2007.

5. Kim W, Porrino JA, Hood KA, Chadaz TS, Klauser AS, Taljanovic MS. Clinical Evaluation, Imaging, and Management of Adolescent Idiopathic and Adult Degenerative Scoliosis. *Curr Probl Diagn Radiol*. 2018;000:1-13. doi:10.1067/j.cpradiol.2018.08.006

6. Heary RF, Albert TJ. *[Spinal Deformities: The Essentials]*. 2 nd. New York: Thieme; 2014.

7. Lee MC, Solomito M, Patel A. Supine magnetic resonance imaging cobb measurements for idiopathic scoliosis are linearly related to measurements from standing plain radiographs. *Spine (Phila Pa 1976)*. 2013;38(11). doi:10.1097/BRS.0b013e31828d255d

8. Davidson N. Measurement and Detection of Radiation by N. Tsoulfanidis. *Med Phys*. 1984;11:732. doi:10.1118/1.595625

9. Yu C, Luxton G. TLD dose measurement: A simplified accurate technique for the dose range from 0.5 cGy to 1000 cGy. *Med Phys*. 1999;26(6):1010-1016. doi:10.1118/1.598493

10. Cristy M. Active bone marrow distribution as a function of age in humans. *Phys Med Biol*. 1981;26(3):389-400. doi:10.1088/0031-9155/26/3/003

11. Computerized Imaging Reference Systems Inc. *Atom Dosimetry Phantoms*.; 2016. http://www.cirsinc.com/file/Products/701_706/701 706 ATOM PB 110615.pdf.

12. IPEM. *Recommended Standards for the Routine Performance Testing of Diagnostic X-Ray Imaging Systems*. 2nd ed. (Hiles P, ed.). Institute of Physics and Engineering in Medicine; 2014.

13. Whitley AS, Sloane C, Hoadley G, Moore AD, Alsop CW. *Clark's Positioning in Radiography*. 12th ed. London: Hodder Arnold; 2005.

14. National Academy of Sciences. *Health Risks from Exposure to Low Levels of Ionizing Radiation: Phase 2, BEIR. VII*. Washington, D.C: National Academy of Sciences; 2006.

15. Ernst C, Buls N, Laumen A, Van Gompel G, Verhelle F, de Mey J. Lowered dose full-spine radiography in pediatric patients with idiopathic scoliosis. *Eur Spine J*. 2018;27(5):1089-1095. doi:10.1007/s00586-018-5561-9

16. Hwang YS, Lai PL, Tsai HY, et al. Radiation dose for pediatric scoliosis patients undergoing whole spine radiography: Effect of the radiographic length in an auto-stitching digital radiography system. *Eur J Radiol*. 2018;108(April):99-106. doi:10.1016/j.ejrad.2018.09.014

17. Wong MD, Wu X, Liu H. The effects of x-ray beam hardening on detective quantum efficiency and radiation dose. *J Xray Sci Technol*. 2011;19(4):509-519. doi:10.3233/XST-2011-0310

18. Ben-Shlomo A, Bartal G, Shabat S, Mosseri M. Effective dose and breast dose reduction in paediatric scoliosis x-ray radiography by an optimal positioning. *Radiat Prot Dosimetry*. 2013;156(1):30-36. doi:10.1093/rpd/nct038

19. Law M, Ma WK, Chan E, et al. Evaluation of cumulative effective dose and cancer risk from repetitive full spine imaging using EOS system: Impact to adolescent patients of different populations. *Eur J Radiol*. 2017;96(July):1-5. doi:10.1016/j.ejrad.2017.09.006

20. Law M, Ma WK, Lau D, Chan E, Yip L, Lam W. Cumulative radiation exposure and

associated cancer risk estimates for scoliosis patients: Impact of repetitive full spine radiography. *Eur J Radiol*. 2016;85(3):625-628. doi:10.1016/j.ejrad.2015.12.032

21. Law M, Ma WK, Lau D, et al. Cumulative effective dose and cancer risk for pediatric population in repetitive full spine follow-up imaging: How micro dose is the EOS microdose protocol? *Eur J Radiol*. 2018;101(February):87-91. doi:10.1016/j.ejrad.2018.02.015

22. Yakoumakis E, Tsalafoutas IA, Nikolaou D, Nazos I, Koulentianos E, Proukakis C. Differences in effective dose estimation from dose-area product and entrance surface dose measurements in intravenous urography. *Br J Radiol*. 2001;74(884):727-734. doi:10.1259/bjr.74.884.740727

23. Tapiovaara M. PCXMC 2.0 Supplementary programs user's guide. 2012;(February).

24. Podnieks EC, Negus IS. Practical patient dosimetry for partial rotation cone beam CT. *Br J Radiol*. 2012;85(1010):161-167. doi:10.1259/bjr/18118287

25. Kim D, Jo B, Lee Y, Park S-J, Lee D-H, Kim H-J. Evaluation of effective dose with chest digital tomosynthesis system using Monte Carlo simulation. 2015;(January 2016):94125D. doi:10.1117/12.2081778

26. Brink RC, Colo D, Schlösser TPC, et al. Upright, prone, and supine spinal morphology and alignment in adolescent idiopathic scoliosis. *Scoliosis Spinal Disord*. 2017;12(1):1-8. doi:10.1186/s13013-017-0111-5

27. Wessberg P, Danielson BI, Willen J. Comparison of Cobb angles in idiopathic scoliosis on standing radiographs and supine axially loaded MRI. *Spine (Phila Pa 1976)*. 2006;31(26):3039-3044. doi:10.1097/01.brs.0000249513.91050.80